Available online at www.sciencedirect.com

SciVerse ScienceDirect

Ceramics International 39 (2013) 3345–3351

CERAMICS INTERNATIONAL

www.elsevier.com/locate/ceramint

Mechanical properties and oxidation behavior of silicon carbide–molybdenum silicides composites

Giuseppe Magnani*, Alida Brentari, Emiliano Burresi, Antonino Coglitore

ENEA, UTTMATF, Faenza Research Laboratories, Bologna Research Center, Via Ravegnana 186, 48018 Faenza, Italy

Received 29 August 2012; received in revised form 5 October 2012; accepted 6 October 2012
Available online 23 October 2012

Abstract

$SiC–MoSi_2$ porous preforms with different $SiC/MoSi_2$ weight ratios were densified by means of the melt infiltration method. Mixture of $SiC–MoSi_2–Mo_{\leq 5}Si_3C_{\leq 1}$ was used as infiltrant. The resultant infiltrated composites showed high density, good mechanical properties and oxidation resistance. In particular, fracture toughness determined at 1773 K was 6.80 MPa $m^{1/2}$ and 6.28 MPa $m^{1/2}$ with SMI-80 (preform with $SiC/MoSi_2$ weight ratio 80/20) and SMI-50 (preform with $SiC/MoSi_2$ weight ratio 50/50) composites, respectively. The same composites showed high temperature (1773 K) flexural strength values: 214 MPa (SMI-80) and 242 MPa (SMI-50). Long term oxidation behavior was also tested at 1773 K and results confirmed the refractoriness of these materials.

Keywords: B. Composites; D. Silicides; D. SiC; Oxidation

1. Introduction

Silicon carbide (SiC) is attractive for high temperature applications due to its low density, excellent high temperature strength and oxidation resistance. On the other hand, the toughness of monolithic SiC is generally low if it is compared to other non-oxide materials (e.g. Si_3N_4). The fracture toughness can be improved by means of crack deflection mechanism in liquid phase sintered SiC (LPS-SiC) [1]. In this case, the addition of additives like Y_2O_3, Al_2O_3, and AlN lead to the formation of grain boundary phases or platelet-like microstructures which are responsible for toughening [1–3]. Another method to increase the fracture toughness of SiC materials is based on the addition of reinforcements [4–6]. Interesting results were obtained with the addition of TiB_2 or TiC [4], but the most promising reinforcement is molybdenum disilicide ($MoSi_2$) due to its high temperature stability and good oxidation resistance [5,6]. $MoSi_2$ was successfully used as reinforcement of silicon nitride to obtain composites with high strength, high toughness and excellent oxidation resistance [7], whereas only limited literature exists on SiC composites reinforced with $MoSi_2$. Different processes have been investigated with the aim to obtain reinforced SiC composites: pressureless sintering [8,9], hot pressing [6,10], reactive sintering [11] and melt infiltration [5,12–15].

Melt infiltration process has been widely used to infiltrate porous preform of SiC using molten Si or molten $MoSi_2$. $MoSi_2$ was selected because it is a very attractive intermetallic compound with a high melting point (2273 K). On the other hand it possesses brittle nature, inadequate creep resistance at high temperature, accelerated oxidation at temperatures between 723 and 823 K and relatively high coefficient of thermal expansion (CTE) compared to SiC. Melt infiltrated $SiC–MoSi_2$ composites were firstly prepared by Lim et al. [12] starting from reaction-bonded SiC preforms. More recently Guo et al. [15] used recrystallized SiC (RSiC) preforms to produce $SiC–MoSi_2$ composites having better oxidation resistance than monolithic RSiC.

Molybdenum carbosilicide (Mo_5Si_3C) is another interesting material in the Mo–Si–C system because it has similar melting point (2373 K), better creep resistance and it is chemically compatible with SiC, C and $MoSi_2$ at high temperature. Zhu and Shobu [16] produced $SiC–Mo_5Si_3C$

*Corresponding author.
E-mail address: giuseppe.magnani@enea.it (G. Magnani).

0272-8842/$ - see front matter © 2012 Elsevier Ltd and Techna Group S.r.l. All rights reserved.
http://dx.doi.org/10.1016/j.ceramint.2012.10.024

composites by melt infiltration of porous preforms obtained by cold isostatic pressing demonstrating that the oxidation of the composites was fairly good up to 1873 K and the strength increased in the range 1473–1873 K due to the brittle–ductile transition of the intermetallic phases.

Finally, Maskaly and Chiang [17] used both $MoSi_2$ and Mo_5Si_3C to produce SiC–$MoSi_2$–Mo_5Si_3C composites using commercial porous preforms (siliconized SiC and continuous SiC fiber composites). They performed the infiltration at 2138 K, but they did not evaluate the effects of the infiltration on the mechanical and oxidation properties of the SiC composites. Based on the above considerations, our work was focused on the evaluation of the mechanical properties and oxidation behavior of melt infiltrated SiC–$MoSi_2$–Mo_5Si_3C composites obtained starting from SiC–$MoSi_2$ porous preforms.

2. Experimental procedure

2.1. Preparation of the SiC–$MoSi_2$ preforms

Commercially available α-SiC (UF15 Premix, H.C. Starck, Germany), $MoSi_2$ (Grade C, H.C Starck, Germany) were used as starting powders. To prepare the preforms, powders of SiC and $MoSi_2$ were mixed in the weight ratio 80–20 (SM-80) and 50–50 (SM-50) with ethanol using Si_3N_4 grinding balls. After drying and sieving, the mixture was compacted by die pressing at 67 MPa and subsequently was pressed at 250 MPa by CIP. The green sample was sintered at 2273 K in a graphite resistance high temperature furnace in flowing argon at 1 atm.

2.2. Preparation of the SiC–$MoSi_2$–Mo_5Si_3C infiltration mixture

Commercially available Mo_2C (H.C. Starck, Germany) and Si (H.C. Starck, Germany) were used as starting powders. On the basis of the study performed by Nowotny et al. [18] on the system Mo–Si–C, the powders were mixed in order to obtain the eutectic composition Si 32 wt%, C 2 wt% and Mo 66 wt%, respectively. The powders were mixed using ethanol and Si_3N_4 grinding balls. After drying and sieving, the mixture was treated at 1773 K in a graphite resistance high temperature furnace in flowing argon at 1 atm.

2.3. Preparation of the composites

The preforms SM-80 and SM-50, obtained on the basis of the procedure described in Section 2.1, were infiltrated with the mixture prepared following the method reported in Section 2.2. The infiltration was conducted using a graphite resistance high temperature furnace. The preforms were completely covered by the infiltration mixture inside a graphite crucible. Infiltration experiments were conducted at 2223 K in flowing argon at 1 atm. The infiltrated composites were identified as SMI-80 and SMI-50.

2.4. Characterization and oxidation tests

The density of the samples was determined by the Archimedes principle (ASTM C373). The microstructures of the samples were observed using scanning electron microscopy (SEM-LEO 438 VP). Compositions were determined by EDS analysis (Oxford Link ISIS 300), while X-ray patterns (XRD) were collected with a Philips powder diffractometer with a Bragg–Brentano geometry and equipped with a copper anode operated at 40 kV and 30 mA (step 0.02°, time 6 s). The phase analysis was carried out with the PC X′pert High Score software Version 2.2a (PANalytical B.V., Almelo, The Netherlands).

The flexural strength was determined by four-point bending tests at room temperature and a T of 1773 K (three samples for each temperature). Samples as bars of $2 \times 2.5 \times 25\ mm^3$ were prepared and tested in accordance with the standard ENV 843-1 (crosshead speed 0.5 mm/min). The fracture toughness was determined by bending bars (three samples for each temperature) of $2 \times 2.5 \times 25\ mm^3$ with a V-shaped notch (SEVNB method in accordance with the standard ENV 14425-5).

Oxidation experiments were carried out at 1773 K over a period of 200 h in air. Square samples (22 mm × 22 mm × 3 mm) were prepared from the bulk specimens with a diamond saw. After grinding to reduce superficial roughness, the specimens were cleaned in an ultrasonic bath and degreased with acetone and ethanol. Dried samples were then weighed and the exact dimensions were measured in order to calculate the surface area. The experiments were conducted in a furnace having molybdenum disilicide heating elements.

3. Results and discussion

3.1. Density, microstructure and crystalline phases

The XRD spectra reported in Fig. 1 confirmed that the infiltration mixture was composed by SiC, $MoSi_2$ and $Mo_{\leq 5}Si_3C_{\leq 1}$ (Nowotny phase). Preliminary infiltration experiments revealed that the infiltrant melts above 2098 K. Spontaneous infiltration was observed at 2223 K and the infiltration process was finished after 15–20 min. SEM images at low magnification of the microstructure of the infiltrated composites (infiltration at 2223 K for 18 min) SMI-50 and SMI-80 are reported in Fig. 2. At higher magnification three phases SiC, $MoSi_2$ and $Mo_{\leq 5}Si_3C_{\leq 1}$ were identified by means of EDS microprobe (Fig. 3). The composites show residual porosity due to some small uninfiltrated zones randomly distributed in the microstructure. In any case, the final density was always higher than 92% T.D. with theoretical density

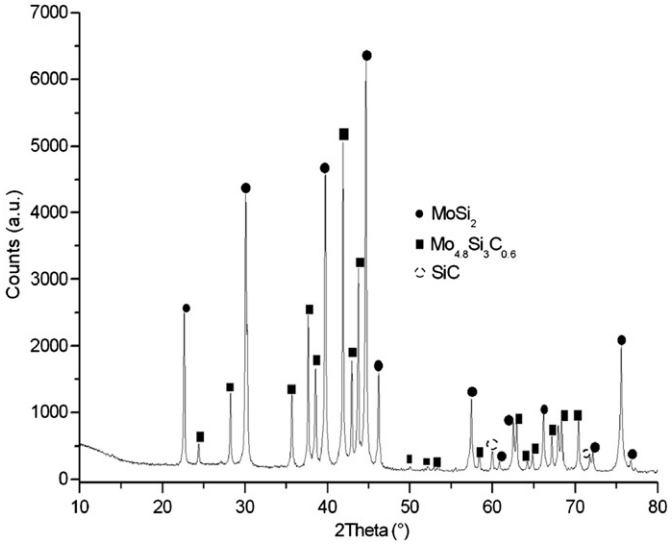

Fig. 1. XRD pattern of the infiltration mixture prepared at 1773 K.

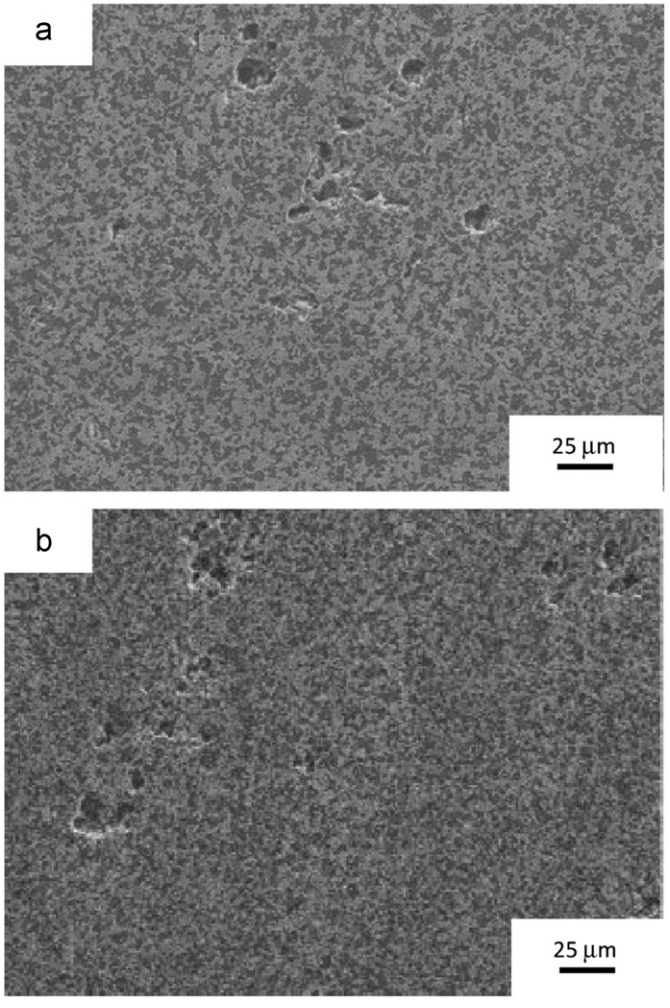

Fig. 2. Low magnification SEM images of (a) SMI-50 and (b) SMI-80 composites (infiltration: 2223 K for 18 min).

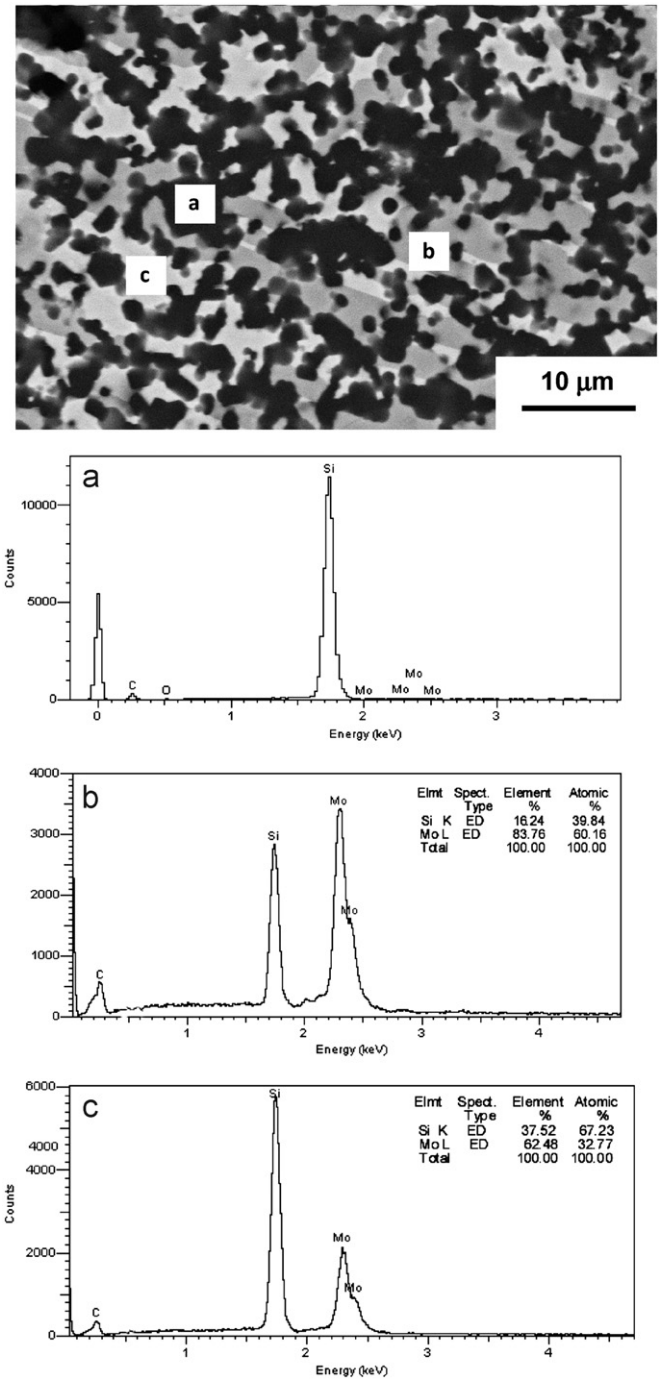

Fig. 3. SEM image of the polished surface of SMI-50 and EDS spectra of (a) SiC, (b) $Mo_{\leq 5}Si_3C_{\leq 1}$ and (c) $MoSi_2$.

of 5.25 g/cm^3 for SMI-50 and 4.95 g/cm^3 for SMI-80 determined by means of the rule of the mixtures using 4.22 g/cm^3, 3.54 g/cm^3 and 6.08 g/cm^3 as theoretical density of SM-50, SM-80 and infiltration mixture, respectively. No cracks were observed in the investigated materials. On the contrary, cracks were observed using preforms with $MoSi_2$ content less than 20 wt% due to the mismatch between the coefficient of thermal expansion (CTE) of SiC and the infiltrant.

3.2. Mechanical properties

Mechanical properties of the infiltrated composites are summarized in Table 1. In the same table, the values of fracture toughness and flexural strength for the hot-pressed $MoSi_2$ [19] and monolithic SiC [20,21] are also reported. The fracture toughness of SMI-80 composite was higher than that of monolithic $MoSi_2$ and SiC, while SMI-50 showed value of fracture toughness similar to monolithic $MoSi_2$ at room temperature with a great increase at high temperature. Fracture toughness of SMI-80 was also higher than that of SMI-50 at room temperature, whereas there was no difference at high temperature. Zhu and Shobu [16,22] and Suresh Kumar et al. [6] obtained similar values of fracture toughness with SiC–Mo_5Si_3C [16], SiC–$Mo_5(Si,Al)_3C$ [22] and SiC–$MoSi_2$ [6] composites. They demonstrated that the increase in toughness at high temperature had to be attributed to the plastic deformation of the reinforcement phases, $MoSi_2$ and Mo_5Si_3C. The plastic behavior induced by the infiltrant mixture in SMI-80 and SMI-50 composites is also evident in the stress–displacement curves reported in Fig. 4. The toughening mechanism is mainly based on the crack bridging since that additional energy is necessary for the plastic deformation and for the crack propagation through the toughening phases [23,24].

The strength increase of the composites at high temperature can also be attributed to the brittle–ductile transition of the intermetallic phases [22,25]. This behavior was particularly evident in SMI-50 composite with high content of intermetallic phases. This composite shows the lowest flexural strength at room temperature, while SMI-80 has higher flexural strength than monolithic $MoSi_2$ at room temperature. In any case monolithic SiC shows always higher strength than infiltrated composites due to the weakness of the silicides.

3.3. Oxidation resistance

The oxidation-induced mass changes of SMI-50 and SMI-80 are plotted as a function of time in Fig. 5a. At the beginning (t=0–5 h), the samples showed a weight loss (Fig. 5b) due to the oxidation of $MoSi_2$ and $Mo_{\leq 5}Si_3C_{\leq 1}$ with consequent evaporation of MoO_3:

$$2\,Mo_5Si_3C + 23O_2 \leftrightarrow 10MoO_3 + 6SiO_2 + 2CO_2 \quad (1)$$

$$MoSi_2 + \tfrac{7}{2}O_2 \leftrightarrow MoO_3 + 2SiO_2 \quad (2)$$

In the range 5–200 h, SMI-50 and SMI-80 composites showed a typical parabolic behavior following the parabolic law:

$$w^2 = kt \quad (3)$$

where w is the specific weight gain and t is the oxidation time. The parabolic constants rate k, determined from the slope of the plot shown in Fig. 6 are reported in Table 2 together to the correlation coefficients. The comparison between the parabolic constants rate of different SiC–$MoSi_2$ [15,26] composites clearly demonstrated that SMI-50 and SMI-80 showed better oxidation resistance without significant difference between the infiltrated composites. The parabolic behavior of the oxidative processes of SiC, $MoSi_2$ and $Mo_{\leq 5}Si_3C_{\leq 1}$ and their composites has been already reported in several studies [15,27–29]. It depends on the diffusion of oxygen through the SiO_2 scale which represents the rate-limiting step. SiO_2 is formed on the basis of the following reactions:

$$5MoSi_2 + 7O_2 \leftrightarrow Mo_5Si_3 + 7SiO_2 \quad (4)$$

$$SiC + \tfrac{3}{2}O_2 \leftrightarrow CO + SiO_2 \quad (5)$$

$$Mo_5Si_3C + xO_2 \leftrightarrow yMo_5Si_3 + zMo_2C + xMo + x2SiO_2 \quad (6)$$

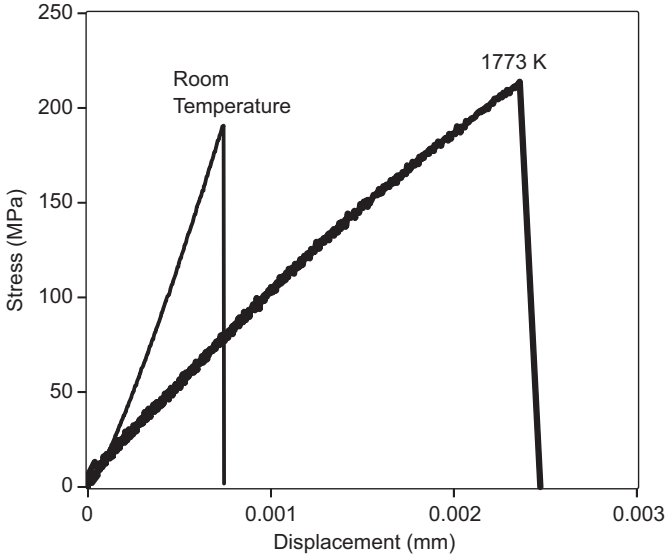

Fig. 4. Stress–displacement curves of SMI-50 tested at room temperature and 1773 K.

Table 1
Fracture toughness and flexural strength of the infiltrated composites and monolithic SiC and $MoSi_2$.

Sample ID	Toughness (MPa $m^{1/2}$)	Flexural strength (MPa)
SMI-80	5.15 ± 0.46 (RT) 6.80 ± 0.34 (1773 K)	191 ± 21 (RT) 214 ± 18 (1773 K)
SMI-50	3.87 ± 0.38 (RT) 6.28 ± 0.44 (1773 K)	113 ± 15 (RT) 242 ± 24 (1773 K)
$MoSi_2$ [19]	4.09 (RT) 0.78 (1673 K)	149 (RT) 149 (1723 K)
SiC [20,21]	2.7 (RT) 2.9 (1573 K)	430 (RT) 430 (1673 K)

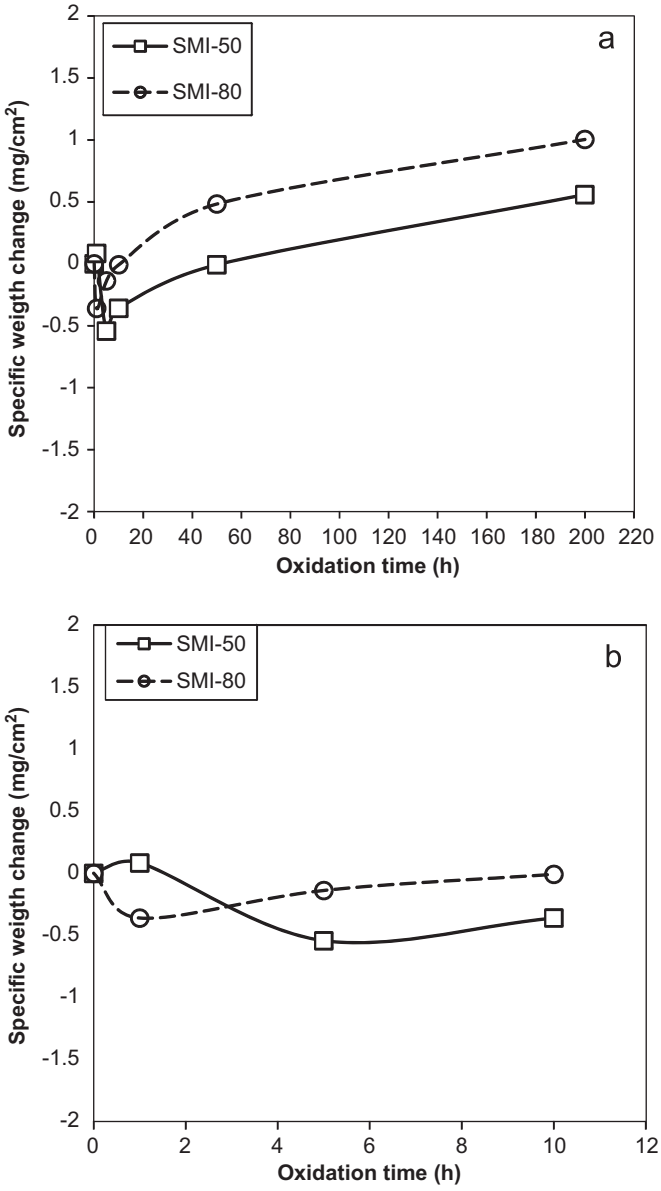

Fig. 5. Specific weight gains of SMI-50 and SMI-80 composites oxidized at 1773 K for (a) 200 h and (b) 10 h.

The oxidation mechanism at high temperature of $Mo_{\leq 5}Si_3C_{\leq 1}$ depends on the partial pressure of oxygen. Zhu and Shobu [27] studied the oxidation behavior of SiC–$Mo_{\leq 5}Si_3C_{\leq 1}$ composites and they concluded that Mo_2C and Mo_5Si_3 are due to the partial oxidation of the Nowotny phase. Mo_2C was revealed by XRD on the surface of the SMI-50 sample oxidized for 200 h (Fig. 7), while the same phase was not detected in SMI-80 after oxidation (Fig. 8). On the contrary, residual $MoSi_2$ was identified in SMI-80, but not in SMI-50. Furthermore, in both the samples Mo_5Si_3 was not detected probably due to the rapid diffusion of Si and/or Mo in $MoSi_2$ which inhibits the achievement of the concentration needed to form Mo_5Si_3 [15].

Finally, in both the samples carbon (graphite) was revealed. This oxidation product is due to the SiC "active" oxidation. The main feature of the "active" oxidation is

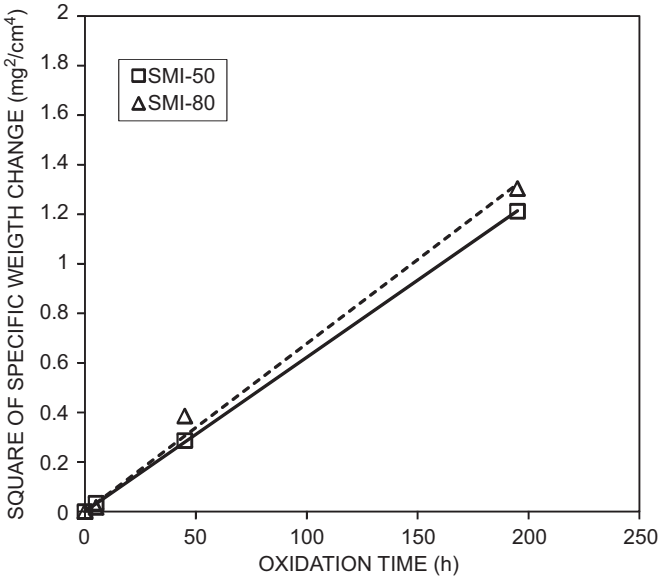

Fig. 6. Square of the specific weight gains of SMI-50 and SMI-80 oxidized at 1773 K.

Table 2
Kinetic constants and correlation coefficients for the oxidation of the investigated materials and analogous materials reported in previous studies.

Sample ID	Parabolic constant rate ($mg^2\,cm^{-4}\,h^{-1}$)	Correlation coefficient
SMI-80	0.007	0.9937
SMI-50	0.006	0.9999
Hot-pressed SiC–$MoSi_2$ (80–20) [26]	0.180	
Recrystallized SiC–$MoSi_2$ (80–20 vol%) [15]	0.100	0.9963

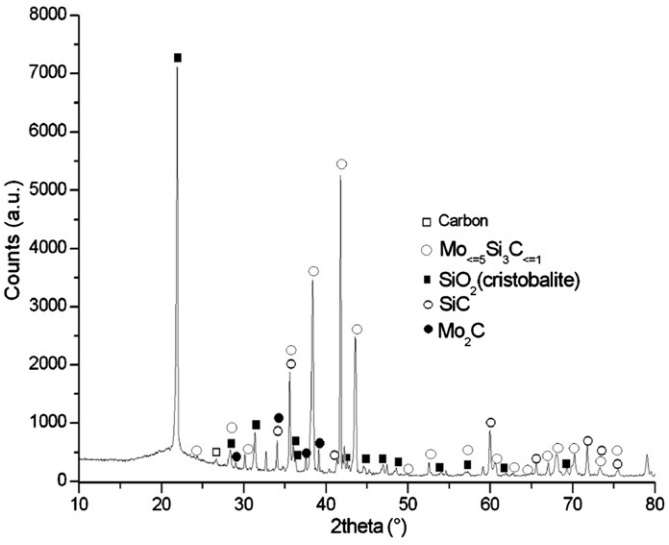

Fig. 7. XRD pattern of the SMI-50 composite after oxidation at 1773 K for 200 h.

the formation of graphite. Previous studies [28,29] on SiC oxidation at very high temperature (≥ 1773 K) reported that the mechanism of the "active" oxidation is based on the following reactions:

$$SiC + O_2 \leftrightarrow SiO + CO \quad (7)$$

$$SiC + O_2 \leftrightarrow SiO_2 + C \quad (8)$$

$$SiO_2 + C \leftrightarrow SiO + CO \quad (9)$$

with graphite formed on the basis of reaction (8). Active oxidation also leads to the formation of volatile species like SiO and CO which could affect the integrity of the protective scale. In the case of SMI-50 and SMI-80 composites, SiC "active" oxidation does not introduce defects (pores and cracks) in the silica layer (Fig. 9). It consequently represents an efficient barrier against inward oxygen diffusion as clearly showed in the oxygen x-ray maps shown in Fig. 9.

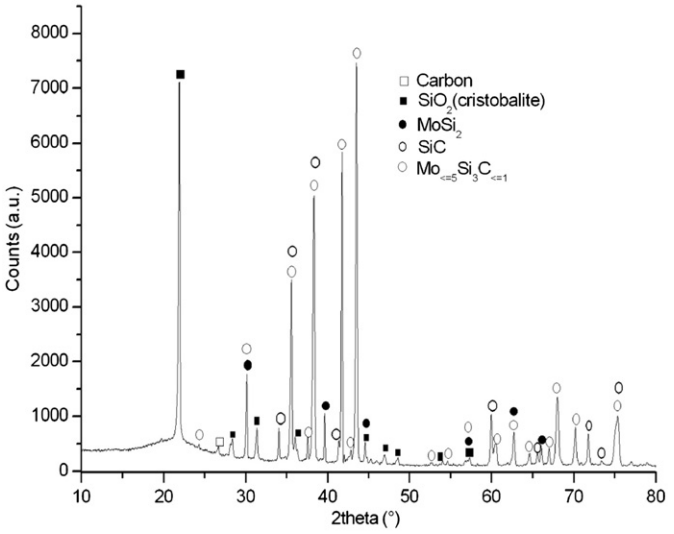

Fig. 8. XRD pattern of the SMI-80 composite after oxidation at 1773 K for 200 h.

4. Conclusion

$SiC–MoSi_2–Mo_{\leq 5}Si_3C_{\leq 1}$ composites were successfully prepared by means of the melt infiltration technique of $SiC–MoSi_2$ preforms. Density was always higher than 92% T.D with uninfiltrated zones homogenously distributed in the sample. The composites showed good mechanical properties (fracture toughness and flexural strength) also at high temperature ($T=1773$ K). Toughness was positively influenced by the presence of intermetallic species like $MoSi_2$ and $Mo_{\leq 5}Si_3C_{\leq 1}$ which acted as reinforcements for the SiC matrix. At the same time, these silicides showed a brittle–ductile transition at high temperature that caused an increase in the flexural strength.

Finally, the composites showed a good oxidation behavior at high temperature. Oxidation mechanism was based on an initial weight loss due to the formation of MoO_3 which finished after the first 5 h of treatment. On the contrary, long term oxidation (from 5 to 200 h) showed a parabolic behavior with very low kinetic rate due to the formation of silica layer that protected the composites against inward oxygen diffusion.

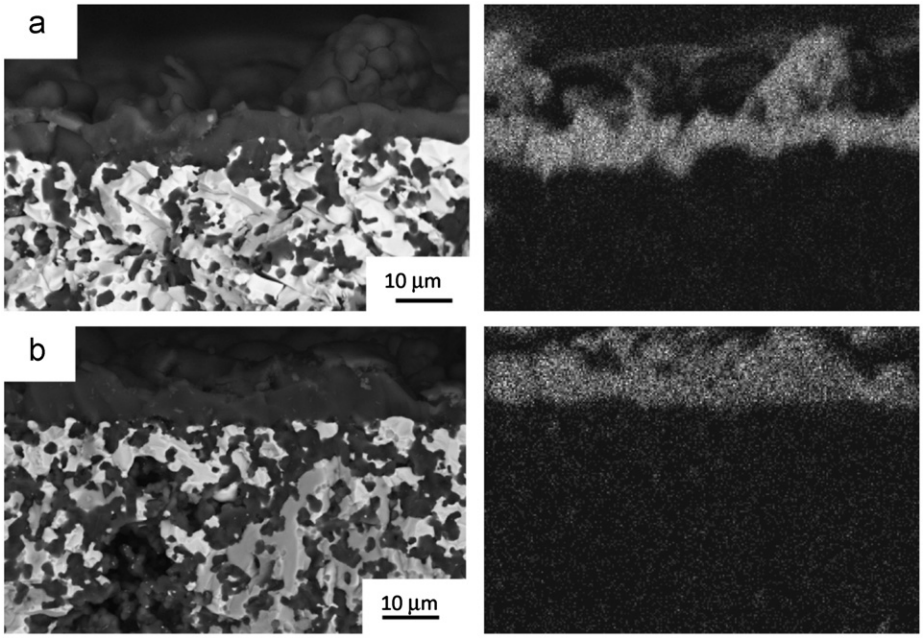

Fig. 9. SEM images of the fracture surfaces and oxygen x-ray maps of (a) SMI-50 and (b) SMI-80 composites after oxidation at 1773 K for 200 h.

References

[1] G. Magnani, L. Pilotti, G.L. Minoccari, Flexural strength and toughness of liquid phase sintered silicon carbide, Ceramics International 26 (2000) 495–500.

[2] J.K. Lee, H. Tanaka, H. Kim, D.J. Kim, Microstructural changes in liquid-phase sintered α-silicon carbide, Materials Letters 29 (1996) 135–142.

[3] G. Rixecker, K. Biswas, I. Wiedmann, F. Aldinger, Liquid-phase sintered SiC ceramics with oxynitride additives, Journal of Ceramic Processing Research 1 (2000) 12–19.

[4] K.S. Cho, Y.W. Kim, H.J. Choi, J.G. Lee, SiC–TiC and SiC–TiB_2 composites densified by liquid-phase sintering, Journal of Materials Science 23 (1996) 6223–6228.

[5] M. Patel, J. Subramanyuam, V.V. Bhanu Prasad, Synthesis and mechanical properties of nanocrystalline $MoSi_2$–SiC composite, Scripta Materialia 58 (2008) 211–214.

[6] R. Suresh Kumar, D. Sivakumar, K. Venkateswarlu, A.S. Gandhi, Mechanical behavior of molybdenum disilicide reinforced silicon carbide composites, Scripta Materialia 65 (2011) 838–841.

[7] M.G. Hebsur, Development and characterization of $SiC_{(f)}/MoSi_2$–$Si3N_{4(p)}$ hybrid composites, Materials Science and Engineering A 261 (1999) 24–37.

[8] D. Sciti, G.C. Celotti, G. Pezzotti, S. Guicciardi, Effect of $MoSi_2$ particles on the fracture toughness of AlN-, SiC-, and Si_3N_4-based ceramics, Journal of Computational Materials 41 (2007) 2585–2593.

[9] F. Chen, J. Xu, Z. Hou, In situ pressureless sintering of SiC/$MoSi_2$ composites, Ceramics International 38 (2012) 2767–2772.

[10] J. Pan, M.K. Surappa, R.A. Saravanan, B.W. Liu, D.M. Yang, Fabrication and characterization of SiC/$MoSi_2$ composites, Materials Science and Engineering 244 (1998) 191–198.

[11] P. Kang, G. Wu, Z. Yin, Influence of Nowonty phase on the fracture toughness of SiC/$MoSi_2$ composites, Key Engineering Materials 353–358 (2007) 1326–1329.

[12] C.B. Lim, T. Yano, T. Iseki, Microstructure and mechanical properties of RB-SiC/$MoSi_2$ composite, Journal of Materials Science 24 (1989) 4144–4151.

[13] R.T. Bhutt, M.G. Hebsur, Processing and properties of SiC/$MoSi_2$–SiC composites fabricated by melt infiltration, Ceramic Engineering and Science Proceedings 21 (2000) 315–322.

[14] O.P. Chakrabarti, P.K. Das, S. Mondal, Study of indentation induced cracks in $MoSi_2$-reaction bonded SiC ceramics, Bulletin of Materials Science 24 (2001) 181–184.

[15] W. Guo, H. Xiao, P. Gao, W. Xie, W. Li, Q. Li, et al., Investigation of $MoSi_2$ melt infiltrated RSiC and its oxidation behavior, Ceramics International 38 (2012) 111–117.

[16] Q. Zhu, K. Shobu, SiC–$Mo_{\leq 5}Si_3C_{\leq 1}$ composites by melt infiltration process, Journal of Materials Science Letters 19 (2000) 153–155.

[17] G.R. Maskaly, Y.M. Chiang, Infiltration processing of transition metal silicide–silicon carbide composites, Ceramic Engineering and Science Proceedings 21 (2000) 307–313.

[18] H. Nowotny, E. Parthe, R. Kieffer, F. Benesovsky, Das Dreistoff-system: molybdan-silizium-kohlenstoff, Monatshefte fur Chemie 85 (1954) 255–272.

[19] S.P. Tantry, S.K. Ramashesa, J.S. Lee, T. Yano, U. Ramamurty, Effect of double reinforcements on elevated-temperature strength and toughness of molybdenum disilicide, Journal of the American Ceramic Society 87 (2004) 626–632.

[20] O.N. Grigor'ev, G.A. Gogotsi, Y.G. Gogotsi, V.I. Subbotin, N.P. Brodnikovskii, Synthesis and properties of ceramics in the SiC–B_4C–MeB_2 system, Powder Metallurgy and Metal Ceramics 39 (2000) 239–250.

[21] H. Klemm, M. Hermann, C. Schubert, High temperature oxidation and corrosion of silicon-based non-oxide ceramics, Journal of Engineering for Gas Turbines and Power 122 (2000) 13–18.

[22] Q. Zhu, K. Shobu, High-temperature mechanical properties of SiC–$Mo_5(Si,Al)_3C$ composites, Journal of the American Ceramic Society 84 (2001) 413–419.

[23] D.R. Clarke, K.T. Faber, Fracture of ceramics and glasses, Journal of Physics and Chemistry of Solids 48 (1987) 1115–1157.

[24] K.S. Ravichandran, The mechanism of toughness development in ductile phase reinforced brittle matrix composites, Acta Metallurgica et Materialia 40 (1992) 1009–1022.

[25] R. Mitra, Mechanical behavior and oxidation resistance of structural silicides, International Materials Reviews 51 (2006) 13–64.

[26] R. Suresh Kumar, D. Sivakumar, A.S. Gandhi, Effect of molybdenum disilicide addtitions on the oxidation behavior of silicon carbide, Scripta Materialia 66 (2012) 451–454.

[27] Q. Zhu, K. Shobu, E. Tani, K. Kishi, S. Umebayashi, Oxidation behavior of $Mo_{\leq 5}Si_3C_{\leq 1}$ and its composites, Journal of Materials Science 35 (2000) 863–872.

[28] E.A. Gulbrunsen, S.A. Jansonn, The high-temperature oxidation, reduction, and volatilization reactions of silica and silicon carbide, Oxidation of Metals 4 (1972) 181–201.

[29] G. Ervin, Oxidation behavior of silicon carbide, Journal of the American Ceramic Society 41 (1968) 347–352.